Supplemental Material

Experimental Procedures

Cloning of *dnrx* Full Length cDNA

A radio-labeled *dnrx* EST (*LP03809*) was used to screen a *Drosophila* 0-20hr embryo cDNA library. Overlapping partial cDNA clones were isolated, sequenced and compiled as a cDNA sequence of 5738 base pairs (GenBank accession number EF460788), which comprises an open reading frame of 5520 base pair with 5' and 3' UTR.

In situ Hybridization

A HindIII-SalI fragment of *dnrx* cDNA clone encoding the 2nd LamG-EGF-LamG-domain repeat, and a PstI-NotI fragment encoding the last-LamG-domain-cytoplasmic-region were cloned into pBluescript vector. The two resulting clones were linearized. Antisense and sense RNA probes were synthesized by using T7 and T3 RNA polymerases, labeled with digoxigenin-UTP (Roche), and used for in situ hybridization following standard protocols.

Production of DNRX Antibody

A guinea pig polyclonal antibody against DNRX was generated against a recombinant protein containing the cytoplasmic region of DNRX fused with a His_6-tag at the N-terminus. The sera were affinity-purified using a recombinant protein containing the same cytoplasmic tail fused to glutathione S-transferase.

The purified anti-DNRX antibody was used at a dilution of 1:500 for tissue staining, and 1:1000 for Western Blot analysis.

Fly Stocks and Genetics

dnrx mutant alleles *dnrx*^{273}, *dnrx*^{241} *and Df(3R)5C1* (a deficiency that removes *dnrx*) were balanced over *TM3 Sb Kr::GFP*. *dnrx* mutants were identified by selecting 3rd instar larvae without GFP expression. *UAS-dnrx* transgenic flies were generated by cloning the entire *dnrx* full-length cDNA into *pUASP* vector for germ line transformation. Gal4 lines used for DNRX overexpression and rescue experiments were *C380*, which drives Gal4 expression mainly in motoneurons (Budnik et al., 1996), and *elav*, which drives Gal4 expression in all neurons (Lin and Goodman, 1994).

Larval Locomotor Assay

The larval locomotor assay was performed as described by Connolly and Tully (1998). Individual larvae were placed in the center of a 145-mm diameter Petri dish, with 3% agar covering the bottom and a 0.5X0.5 cm square grid marked on the lid. The number of grid line crossings within a 30 second time window was recorded six times.

Generation of *dnrx* Mutants

XP d08766 (Thibault et al., 2004), a P-element inserted ~200bp upstream of *dnrx*, was used to carry out an excision screen. To increase the frequency of

large deletions, the excision screen was carried out in *mus309* background (Adams et al., 2003; McVey et al., 2004). Briefly, *XP d08766* was first recombined to *mus309*^{N1}. *mus309*^{N1} *XPd08766/TM6 Tb* males were massively mated with *mus309*^{D3} *Sb* ∆*2-3/TM6 Tb* females. The *mus309*^{N1} *XPd08766/mus309*^{D3} *Sb* ∆*2-3* males were individually crossed with *D/TM6 Tb* females. *w*$^{-}$ male progeny was selected and individually crossed with *Df(3R)5C1/TM3 Sb Kr::GFP.* Single ∆*XP/ Df(3R)5C1* male flies were subject to PCR to select imprecise excisions, and ∆*XP/ TM3 Sb Kr::GFP* were used to establish stock lines. *dnrx* deletions were obtained by selecting imprecise excisions downstream of the P-element insertion site using primer pairs covering the whole *dnrx* locus. The following primer pairs were used to confirm *dnrx*^{273} and *dnrx*^{241} alleles with a common 5'primer (5'-ACGCGTCGCGCTAAAATCCAGCCCG-3'); and separate 3' primers (*dnrx*^{273}, 5'-CGTATGAGTGCTTGGAGCGGAA-3'; and *dnrx*^{241} , 5'-AGCCGGTGCCGATGTCTATGACGAA-3').

Immunohistochemistry, Confocal Microscopy, and Morphological Quantification

Preparation and antibody staining for whole-mount embryos and dissected wandering 3rd instar larvae were performed as described by Bellen and Budnik (2000). Dissected larval NMJs were fixed in Bouin's fixative for 15 min. The following antibodies were used: guinea pig anti-DNRX (1:500), rabbit anti-DPAK (1:2000, N. Harden, Simon Fraser University, Canada; Harden et al., 1996),

rabbit anti-NWK (1:2000, B. Ganetzky, University of Wisconsin, Madison; Coyle et al., 2004), rabbit anti-Syt I (1:500, H. Bellen, Baylor College of Medicine, Houston; Littleton et al., 1993); rabbit anti-GluRIII (1:2000, A. DiAntonio, Washington University, St. Louis; Marrus et al., 2004); guinea pig anti-Dap160 (1:2000, H. Bellen, Baylor College of Medicine, Houston; Koh et al., 2004), monoclonal anti-DLG (1:500), anti-BRP (1:500), anti-GluRIIA (1:50), and anti-FASII (1:100) from Developmental Studies Hybridoma Bank, University of Iowa. Secondary antibodies conjugated to Alexa 488, 568 and 647 (Invitrogen-Molecular Probes) were used at 1:400. Fluorescence conjugated anti-HRP (Jackson Immuno Labs) antibodies were used at 1:50.

DNRX signal at the NMJ was detected by using the VECTASTAIN ABC system (Vector Laboratories) and Tyramide Signal Amplification (TSA, Invitrogen-Molecular Probes). Double-staining of NMJ with anti-DNRX and a second primary antibody was performed as following. Briefly, fixed larvae were washed in PBT (PBS containing 0.3% Triton X-100) and blocked for 1hr with 1% blocking reagent (TSA kit, Invitrogen-Molecular Probes). Blocked samples were incubated with anti-DNRX and a second primary antibody overnight at 4 °C. After washes with PBT, the samples were incubated with biotinylated goat anti-guinea pig antibody (1:400, Vector Laboratories) and a fluorescent secondary antibody. The incubation was followed by washes with PBT and one-hour incubation in ABC reagent (1:250 in 2% BSA /PBT, diluted 30 min before use, Vector laboratories). Six subsequent washes with PBT and one with PBS were followed by Tyramide labeling according to the manufacturer's instructions.

Confocal images were acquired using a Bio-Rad Radiance 2000 confocal microscope with LaserSharp2000 software. Samples for each experiment were processed simultaneously, and imaged using the same settings. For Cac-GFP live imaging, larvae were mounted on the slides and the images were acquired from live body wall muscle preparations with an Improvision spinning disc confocal microscope.

Quantification of bouton number was performed at muscles 6/7 and muscle 4 of abdominal segment 3. Total boutons at NMJ6/7 and type Ib boutons at NMJ4 were visualized by staining of body wall muscle preparations with anti-HRP. For quantification of axonal Syt accumulation, the length of SNb axon innervating muscles 12/13 or ISN axon and its primary branches innervating muscle 4 in abdominal segment 3 or 4 was measured; the number of Syt puncta along these axons was counted and further divided by the axon length. Statistical analyses were performed using InStat 3.00 (Graphpad).

Electron Microscopy

Body wall muscles were prepared for TEM as previously described (Torroja et al., 1999). Synaptic boutons were serially sectioned and photographed at 10,000-30,000X using a JEOL 100S TEM. For morphometric analysis, the cross section corresponding to the bouton midline (cross-section of largest diameter) was identified, the negative scanned at 60,000X, and used for quantification using Image J as in Budnik et al., 1996. The number of samples used were 3 wild type controls (14 boutons), 3 *dnrx/Df* (11 boutons), and 3 rescue animals (15

boutons). For analysis of synapse length and synapse ruffles sections other that the midline section were also considered for quantification, as long as pre- and postsynaptic densities, as well as the synaptic cleft were clearly visualized, had consistent thickness, and lacked the blurry appearance of membranes cut at a tangential plane. Statistical analysis was performed using a two-tailed Student t-test.

Electrophysiology

Electrophysiology recordings were performed as in Ashley et al., 2005. Briefly, third instar larvae were dissected under cold 0.3mM Calcium HL-3 saline and then perfused continuously with 0.5mM Calcium HL-3 saline at 22°C. Muscle 6 in segment A3 was then impaled with a 15-20 MΩ glass electrodes. Only samples with resting membrane potentials between -60 mV and -63 mV were used for analysis. Data was collected using an Axoclamp2A (Molecular Devices), filtered at 1 kHz, and digitized with an Instrutech (Port Washington) ITC-16 computer interface using Pulse software (HEKA Electronik, Lambrecht/Pfalz). Spontaneous and evoked events were then measured using Mini Analysis software (Synaptosoft). Statistical analysis was performed using the Student's t test.

Quantification of GluR IIA Intensity

NMJ staining of *dnrx* mutant and wild-type larvae with monoclonal anti-GluRIIA and FITC anti-HRP was performed in the same tube. Several regions of NMJ4

from 3 animals for each genotype were scanned by confocal microscope. Confocal stacks were acquired using the same settings that prevented pixel saturation with 0.25 μm steps through entire synaptic boutons. Images were processed using Volocity 4.1 (Improvision). Total volumes of synaptic boutons outlined by HRP staining, and the fluorescence of GluRIIA staining were calculated. Total GluRIIA fluorescence divided by total volumes of boutons represented GluR intensity.

Supplemental Figures

Fig. S1. Distribution of Active and Periactive Zone Proteins in *dnrx* Mutants

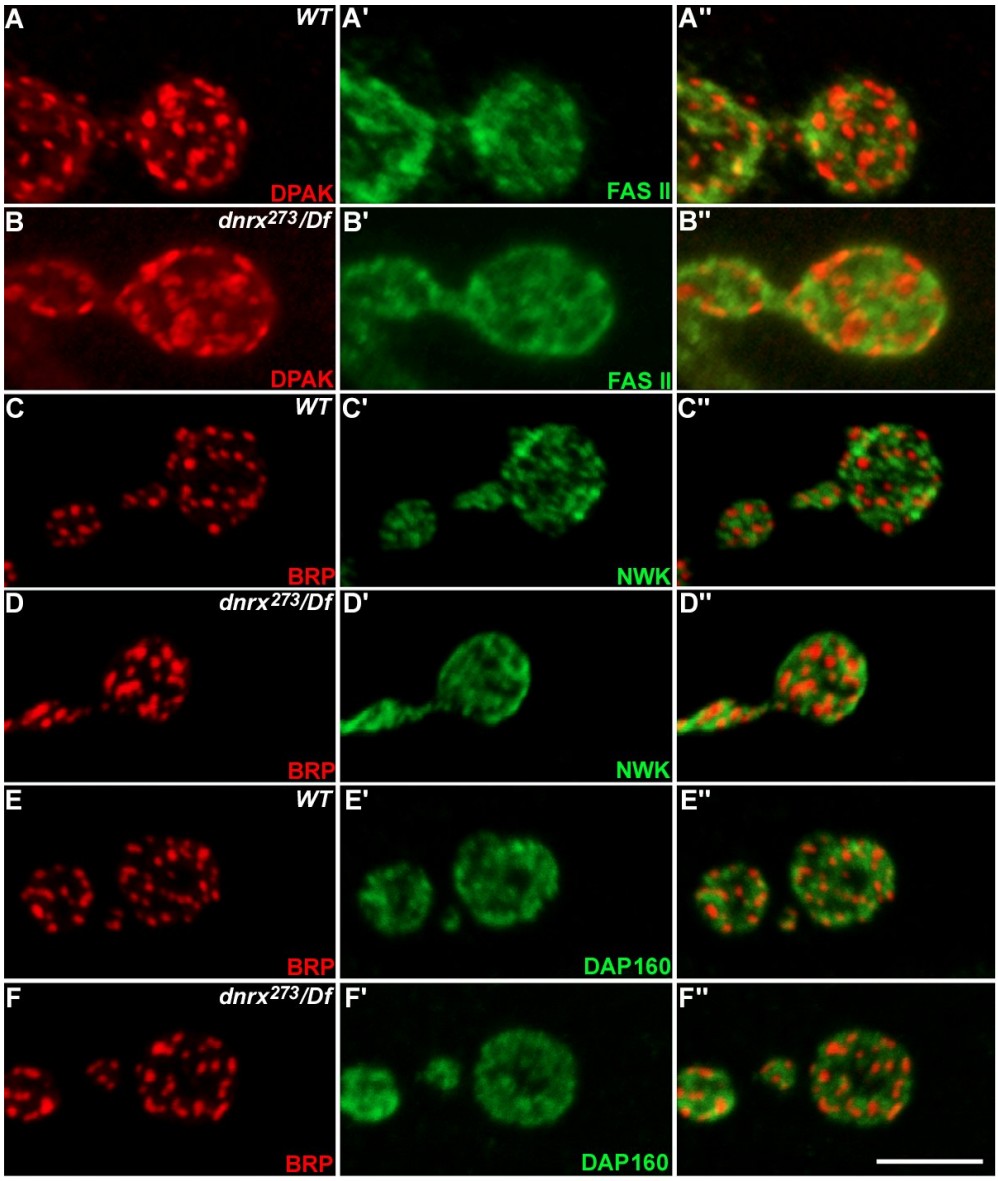

Synaptic boutons of wild-type (A-A'', C-C'' and E-E'') and *dnrx* mutants (B-B'', D-D'' and F-F'') double-stained for active zone (DPAK and BRP, red) and periactive zone markers (FASII, NWK and Dap 160, green). Mutant boutons have a increased distribution of DPAK (B). The cell adhesion molecule FASII, the cytoskeleton adaptor protein NWK and the endocytotic protein Dap 160 surrounding the active zone proteins have a similar distribution in *dnrx* mutants (B'-B'', D'-D'', and F'-F'') as in the wild-type (A'-A'', C'-C'' and E'-E''). Scale bar: 5μm

Fig. S2. Distribution of Postsynaptic GluRIIA in *dnrx* Mutants.

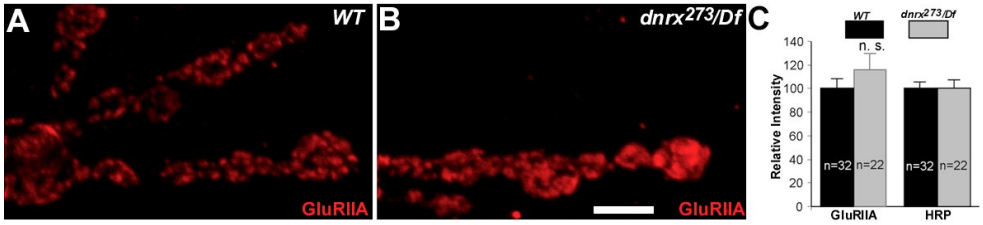

NMJ staining for GluRIIA in wild-type (A) and *dnrx* mutants (B). Note that the distribution of GluRIIA clusters is increased in *dnrx* mutants.

(C) Quantification of GluRIIA fluorescence intensity in synaptic boutons. HRP is the internal control. Relative intensity is expressed as percent of wild type level. No significant difference is observed between mutant and wild-type boutons. Data are mean±SEM. Scale bar: 5 μm.

Fig. S3. Distribution of Presynaptic N-type Calcium channels at the NMJ.

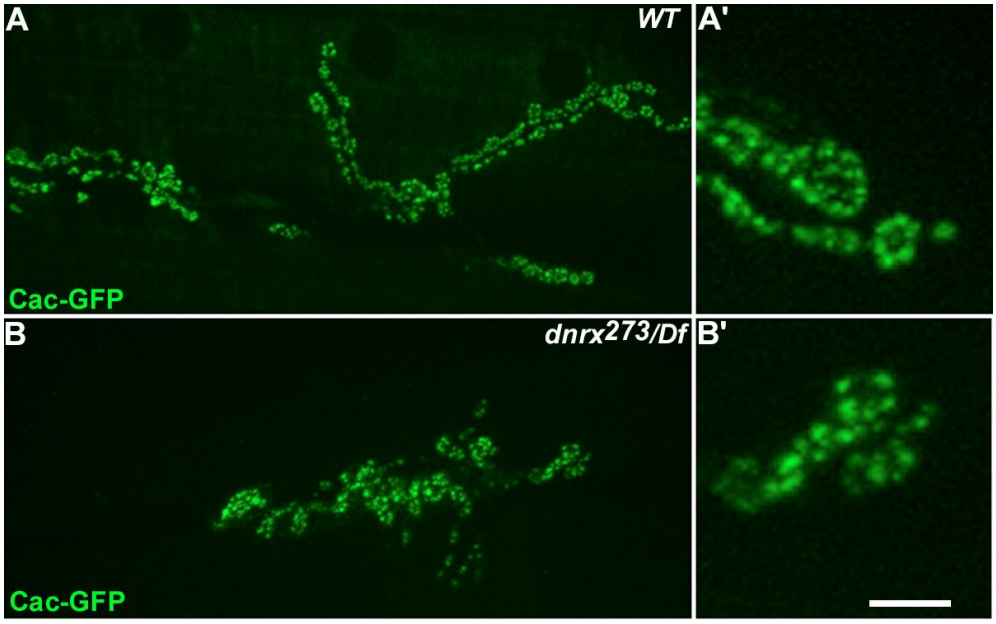

(A, B) Confocal images of NMJ6/7 in preparations expressing Cac-GFP in neurons and imaged live in wild type (A and A'), and *dnrx* mutants (B and B'). No significant changes in the intensity of the signal between the two genotypes were found (WT: 100±1.4, n=9; $dnrx^{273}/Df$: 97.9±1.2, n=6). Scale bar: A, B, 17 µm; A', B', 4 µm.